The Ultra-Low Friction of Layer Structures

Michail V. Nozhenkov[1]

[1] Russian Academy of Sciences, Joint-Stock Company "Technom-T", Moscow, Russia

Correspondence: Michail V. Nozhenkov, Russian Academy of Sciences, Joint-Stock Company "Technom-T", Warsaw highway, d.126-453, Moscow 117587, Russia. Tel: +7(495)585-91-27; +7(495)315-62-51. E-mail: technomt@technom-t.ru

Abstract

The article investigates the process of obtaining the properties of thin films of layered materials, applied vacuum ion-plasma deposition methods. A study of the tribological properties was performed electron diffraction and electron microscopy studies of the structure. It was found a positive effect of the deposition of wear-resistant sublayer and alloying of the antifriction layer, which led to a considerable increase endurance and appearance of ultra-low (super-low) friction. The generalized model of crystal growth mechanism and ultra-low friction, which is based on the possibility of mass transfer non-dissipative (energy) in the absence of resistance forces during the move. Also found that the ultra-low (super-low) friction, superconductivity and superfluidity are related phenomena defined by the phase transition of the energy distribution of particles through a critical value (energy potential barrier). Energetically favorable arrangement of the particles in the crystal lattice of the lattice for the realization of the non-dissipative movement with the disappearance of forces of resistance are the Van der Waals areas, which is followed by predicting the implementation of the investigated phenomena.

Keywords: vacuum ion-plasma sputtering, doped coatings, ultra-low (super-low) friction

1. Introduction

To protect work surfaces and improve the physical and mechanical properties of the surface layers are applied anti-friction wear-resistant coatings deposited by various methods. Modern high-tech industries, which require the use of accurate low-friction running clearance required the creation of new technologies for applying thin coatings to protect sliding surfaces from wear. Features of the crystal structure and anisotropy in different crystallographic directions led to the use for these purposes dichalcogenides of transition metals (Bulaevskii, 1975).

Particularly relevant is the protection of friction pairs, made from materials that are prone to setting, followed by catastrophic wear (especially in a high vacuum). Austenite stainless steel and titanium alloys are among these materials. Vacuum ion-plasma methods of applying such coatings based on ion (cathode) sputtering, have a number of advantages. Coatings deposited by cathodic sputtering, have high adhesion to a substrate, maintaining the stoichiometry of uniformity of distribution and uniformity in thickness. When changing the process conditions applied in the preparation of ion-vacuum plasma coating becomes possible to form different crystal structures and, consequently, the change in their physical, mechanical and tribological characteristics. Thus, the development of technology allows you to manage the process of producing coatings and create the desired properties (Nozhenkov, 2012a, 2012b, 2013a, 2013b, 2013c, 2014).

1.1 Goal of the Work

The work is aimed at establishing the effect of applying process conditions on the crystalline structure of coatings based on the dichalcogenide of transitional metals of groups IV–VI obtained by the vacuum ion-plasma methods and on their t tribotechnical properties.

1.2 Objects and Methods of Studies

Polished specimens from compact ceramics Al_2O_3, SH-15 steel and 12X18H10T steel served as substrates for application of coatings. The substrates were coated with molybdenum disulfide and diselenide (MoS_2, $MoSe_2$) and tungsten disulfide and diselenide (WS_2, WSe_2). The method of applying the coatings with ion-plasma sputtering is described in (Nozhenkov, 2012a, 2012b, 2013a, 2014). The coatings were applied at a substrate

temperature of 283–1573 K. The crystalline structure of coatings was studied with an EMR-102M electronograph, and the surface morphology was studied with JXA-841 and JSM-35C electron microscopes. The elementary composition of the obtained coatings was explored with JEM-100C instruments that have the attachment CEVEX by spectroscoping the typical X-ray emission and ESCALAB-5, which performs photoemission spectroscopy by X-ray excitation.

The tribotechnical tests were carried out in air under normal conditions in UGS-1 tribapparatuses with the disk-on-sphere MPC-1 specimens (the end-face friction with periodic contacting). The disk-on-sphere tests (UGS-1) with a sphere diameter of 9.0 mm were carried out under a load of 3.0 N, the sliding velocity was constant to be equal to 0.019 m/s. The durability criterion as applied to disk-on-sphere tests; the coating was considered unfit if the coefficient of friction was less than 0.1. The end-face friction tests (MPC-1) were performed by periodic contacting with a cycle duration of 1.2 s when the specimens were 0.4 s in contact. The maximum load was 3.0 N, the sliding velocity during tests was constant (0.031 m/s at the specimen r.p.m. = 0.75 rev/s), and the tests lasted 20,000 contact cycles (Nozhenkov, 2013b).

2. Experimental Results

2.1 The Influence of the Deposition Temperature

It is revealed that MoS_2 coatings appear when the substrate temperature changes on the specimens from compact ceramics Al_2O_3. The coatings have the following structures:

- quasi-amorphous (at T < 383 K);

- polycrystalline disordered;

- polycrystalline textured with predominant orientations along axes of crystallites $[10\bar{1}0]$ (at T = 473–573 K and T = 773–923 K) and $[11\bar{2}0]$ (at T = 673–773 K) perpendicular to the substrate surfaces (Figure 1). All crystalline coatings have a hexagonal type $2H$–MoS_2 structure.

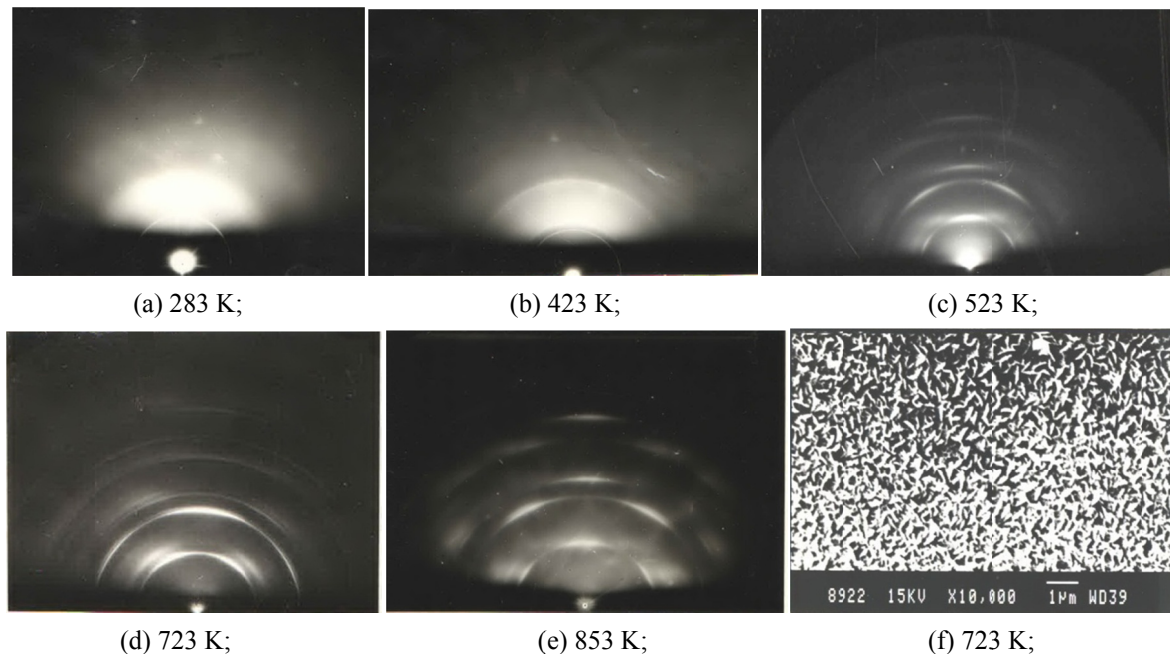| (a) 283 K; | (b) 423 K; | (c) 523 K; |
| (d) 723 K; | (e) 853 K; | (f) 723 K; |

Figure 1. (a–d) Electronograms and (f) microphotogaph of MoS_2 coatings applied at various substrate temperatures: (a) 283 K; (b) 423 K; (c) 523 K; (d) 723 K; (e) 853 K; (f) 723 K

The disk-on-sphere specimens were tested in order to determine the tribotechnical properties of MoS_2 coatings (Figure 2). The electronograph studies (Figure 1) and durability tests (Figure 2) show that the most optimum coatings are those with the highest degree of structural perfection oriented along the axes of crystallites $[10\bar{1}0]$ within the temperature range of 450–850 K. When the temperature grows above 900 K, the durability will decline.
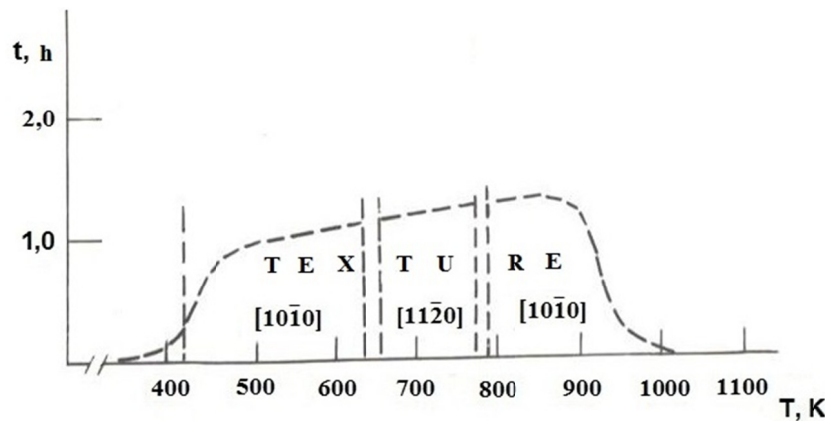
Figure 2. Dependence of durability of MoS_2 coatings applied on Al_2O_3 specimens on substrate temperature during deposition, for triboengineering tests of disk-on-sphere couples

2.2 Changes in the Structure of Coatings During Friction

Coatings 0.5×10^{-6} m thick were applied to Al_2O_3 specimens by DC and high-frequency sputtering at a substrate temperature of 523 K to further investigate the effect of the potential type of sputtering and the processes that evolve the surface layers of MoS_2 coatings in friction. After application, the disk-on-sphere couples were subjected to tribotechnical tests of various durations in the UGS-1 triboapparatus and end-face friction tests were performed in the MPC-1 triboapparatus; in addition, changes in the crystalline structure were studied in friction. The end-face friction tests were selected because the electronographic studies fail to reveal the structure when the friction surface is in the friction path groove.

The electronographic studies did not reveal any noticeable changes in the initial texture at the beginning of the test (Figure 3a). The coefficient of friction during end-face friction tests was rather high in the beginning (0.26–0.27, Figure 4b). The coefficient of friction during disk-on-sphere tests was considerably smaller (Figure 4a). As the cycles prolong to 10 (Figure 3a), in addition to the diffraction texture pattern with the axis [1010], the electronograms show weak traces of reflection, which proves that the texture appears with the axis [0001] perpendicular to the substrate surface. The coefficient of friction somewhat diminishes (0.24–0.25, Figure 4b).
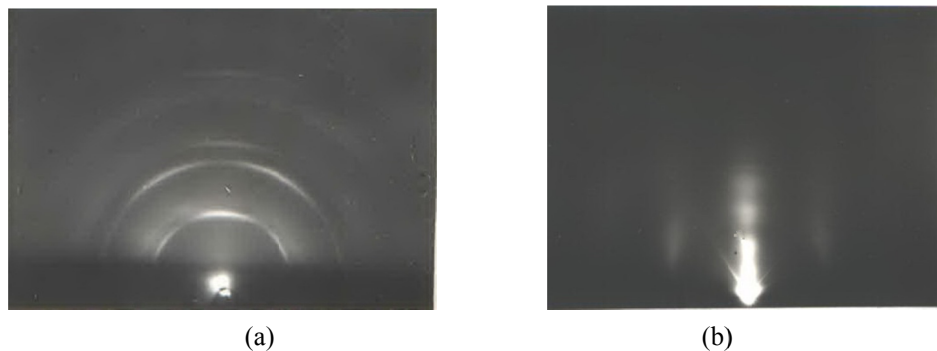

(a)   (b)

Figure 3. Electronograms of MoS_2 coatings after tests of different duration (number of contacting cycles): (a) 10; (b) 10,000 contact cycles
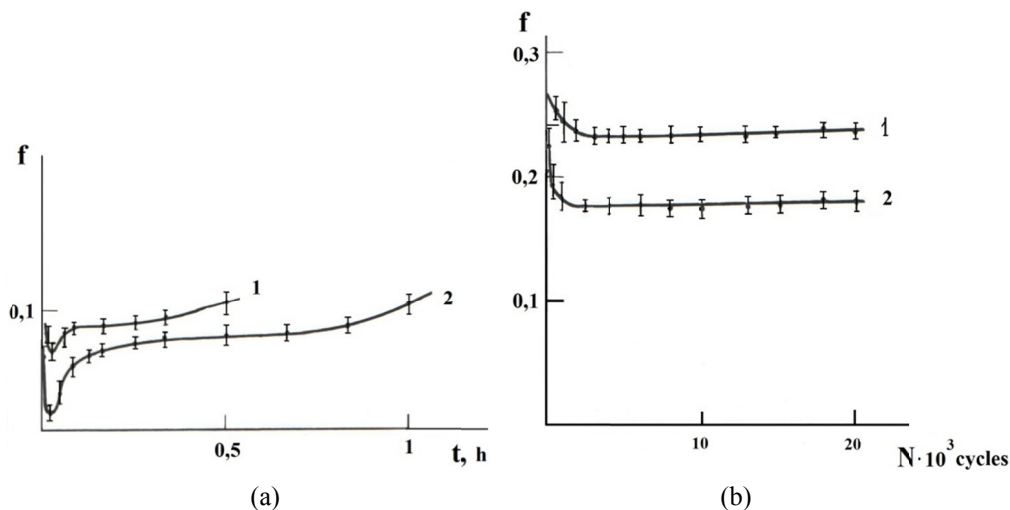
Figure 4. Dependence of coefficient of friction on duration of tests of MoS_2 coatings applied by DC sputtering (1) and high-frequency sputtering (2): (a) disk-on-sphere couples (UGS-1); (b) end-face friction couples (MPC-1)

After 100 cycles, relatively distinct reflexes (0002), (0004), and (0006) appear that correspond to the texture with the axis [0001]. It proves that a layer was formed with the predominant crystallite orientation along the axis [0001] perpendicular to the substrate surface on the electronograms of friction tracks. Apparently, the appearance of the diffraction pattern that correspond to the texture [0001] is due to a thicker and more perfect surface layer formed on the MoS_2 coating under the effect of friction forces. During this period, the coefficient of friction diminishes from to 0.2 (Figure 4b). When the friction tests last longer during end-face tests, (Figure 4b) up to 200–300 cycles, the coefficient of friction stabilizes at a level of 0.18–0.19. Afterwards, the coefficient of friction remains nearly unchanged. After tests lasting 1000 cycles, electronograms from the coating surface show a clear pattern with diffraction maxima (0002), (0004), (0006), (0008), etc., which proves that there is a texture of crystallites with the axis [0001] perpendicular to the substrate surface. The diffraction pattern from underlying layers with the texture [1010] is hardly observed, which proves that there is a texture of crystallites with the axis [0001] perpendicular to the substrate surface. The diffraction pattern from underlying layers with the texture [10 10] is hardly observed, which proves the significant thickness of the layer with the texture formed on the coating surface under the effect of friction force. Since the permeating capacity of the electron beam is approximately 0.5×10^{-8} to 1.0×10^{-8} m, the layer thickness with the texture [0001] should apparently be smaller than these values.

The growth of cycles to 10,000 leads to the formation of a more pronounced texture with the axis [0001] on the friction track. The electronogram (Figure 3b) shows the diffraction maxima with indexes (0001), which prove the location of MoS_2 with the base plane (0001) parallel to the friction surface. The studies have revealed that the friction tests in the MPC-1 trioapparatus under the effect of friction forces; the angular disorientation of crystallites with the texture [1010] perpendicular to the substrate surface diminishes (Figure 5a). This layer thickens in the process of friction and reaches during tests that last up to 10,000 cycles to approximately 0.5 to 1.0×10^{-8} m. If a base plane (0001) with a smaller surface energy orients parallel to the substrate surface, it ensures the most optimal geometry of arrangement of crystallites and, therefore, a lower coefficient of friction.

The substrate temperature effect was studied during the application of coatings, the formation of the structure, and placement in the center and over the periphery over the plate, holding substrates, on the crystalline structure and the tribotechnical properties in order to disclose the structure obtained during application and the properties of coatings based on other dichalcogenides ($MoSe_2$, WS_2, WSe_2).

(a)   (b)
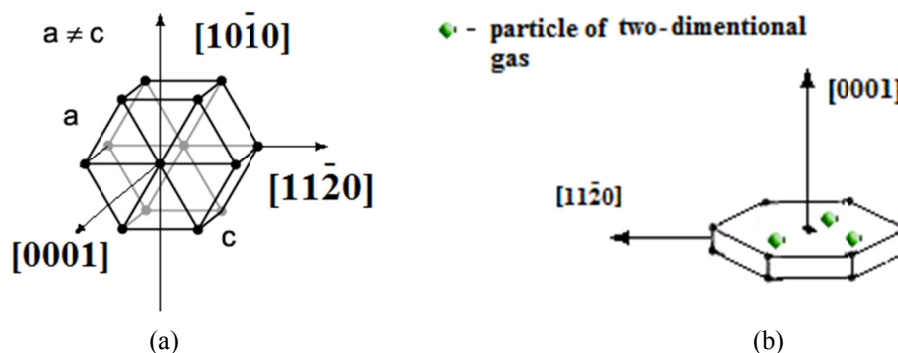
Figure 5. Diagram of crystallographic directions of hexagonal MX$_2$ lattice in textures of coatings before (a) and after (b) friction tests

2.3 The Influence of the Deposition Temperature on the Structure of Other Dichalcogenides

It is established that substrate temperature changes produce the formation of coatings with the structures similar to the MoS$_2$ structure with crystallites oriented along the axis [1010] perpendicular to the substrate surface (for MoSe$_2$, WS$_2$, WSe$_2$) for the temperature range (473–973 K) and to the axis [1020] (for MoS$_2$ at T = 673–773 K) (Figures 6, 7). The lowest temp of crystallization is observed among the coatings from MoS$_2$ (at T = 383 K) (Figures 2, 8), while the highest one for WSe$_2$ (Figure 8). Works (Nozhenkov, 2012a, 2012b, 2013a, 2014) show that textures with the [1010] axis grow among all dichalcogenides, while the texture with [1120] revealed growth among the coatings from MoS$_2$ in the temperature range of 673–773 K. The [0001] axis was fully disoriented in the plane parallel to the substrate surface. The coincidence of the electron beam direction in the electronograph column with the radius from the plate center leads to the resulting symmetric diffraction pattern, the mage under the beam displaces parallel and the pattern remains unchanged (Figures 6a–6d, 7a–7d). Away from the periphery, the axis [1010] inclines smoothly towards the center; simultaneously, the axis [0001] orients over the radii of the specimen holder and the inclination angle reaches ~30°. The obtained results are confirmed by the study of the morphology of surfaces coatings (Figures 7d–7g); the microphotographs show that the crystallites orient almost regularly with some angular scatter that ensures the formation of the texture type diffraction pattern. The crystallites away from the plate center form closed concentric circumferences. This growth regularity is maintained during the application of coatings of other molybdenum and tungsten dichalcogenides (e.g., MoSe$_2$, WS$_2$, WSe$_2$) (Figures 6d–6g, 7d–7g).
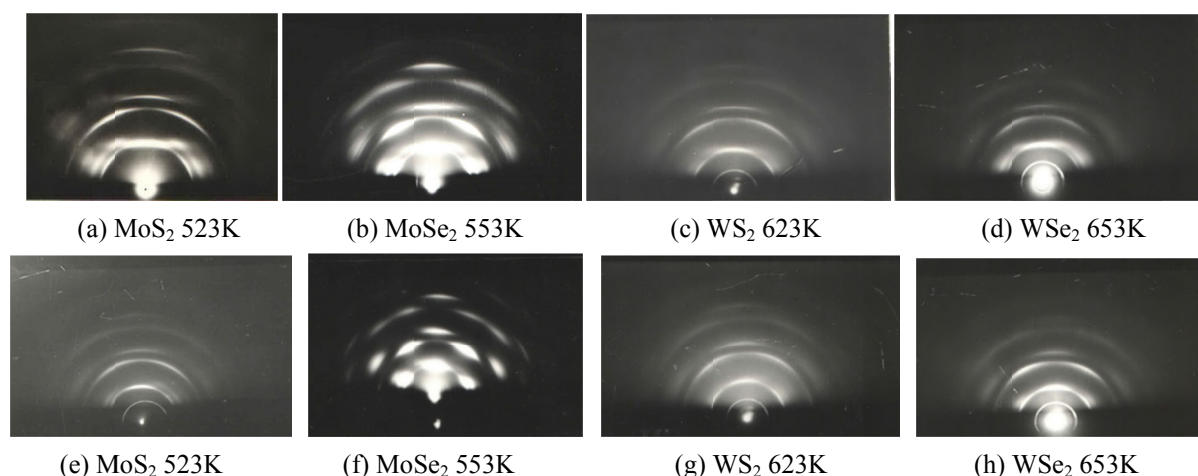

(a) MoS$_2$ 523K   (b) MoSe$_2$ 553K   (c) WS$_2$ 623K   (d) WSe$_2$ 653K

(e) MoS$_2$ 523K   (f) MoSe$_2$ 553K   (g) WS$_2$ 623K   (h) WSe$_2$ 653K

Figure 6. Electronograms of (a, e) MoS$_2$, (b, f) MoSe$_2$, (c, g) WS$_2$, and (d, h) WSe$_2$ coatings applied at a temperature of 523 K (MoS$_2$); 553 K (MoSe$_2$); 623 K (WS$_2$); 653 K (WSe$_2$) when specimens were located (a-d) at the center of the plate and (e–g) over the periphery
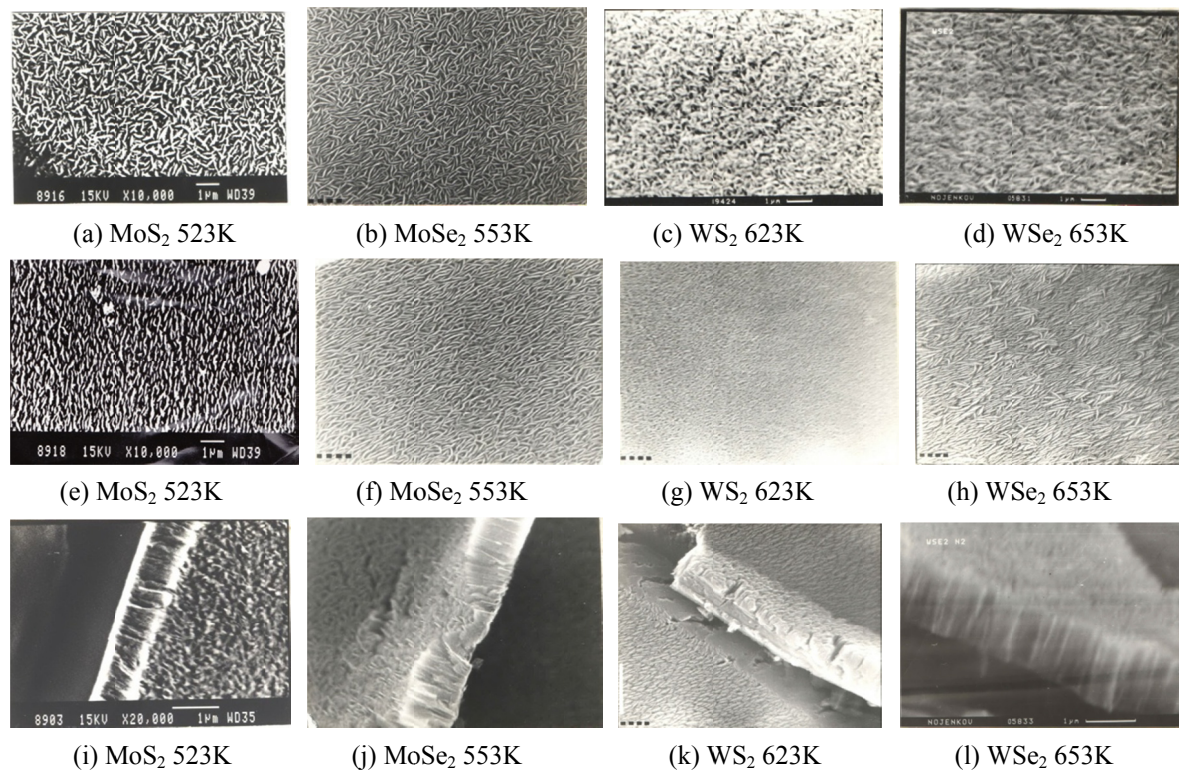
(a) MoS$_2$ 523K	(b) MoSe$_2$ 553K	(c) WS$_2$ 623K	(d) WSe$_2$ 653K
(e) MoS$_2$ 523K	(f) MoSe$_2$ 553K	(g) WS$_2$ 623K	(h) WSe$_2$ 653K
(i) MoS$_2$ 523K	(j) MoSe$_2$ 553K	(k) WS$_2$ 623K	(l) WSe$_2$ 653K

Figure 7. Microphotogaph of (a–e) surface and (i–m) spall of (a, d, i) MoS$_2$, (b, g, k) MoSe$_2$, (c, e, l) WS$_2$, and (d, g, m) WSe$_2$ coatings applied at temperature 523 K (MoS$_2$); 553 K (MoSe$_2$); 623 K (WS$_2$); 653 K (WSe$_2$) when specimens are located (a–d) at the center of the plate center and (e–g) over periphery
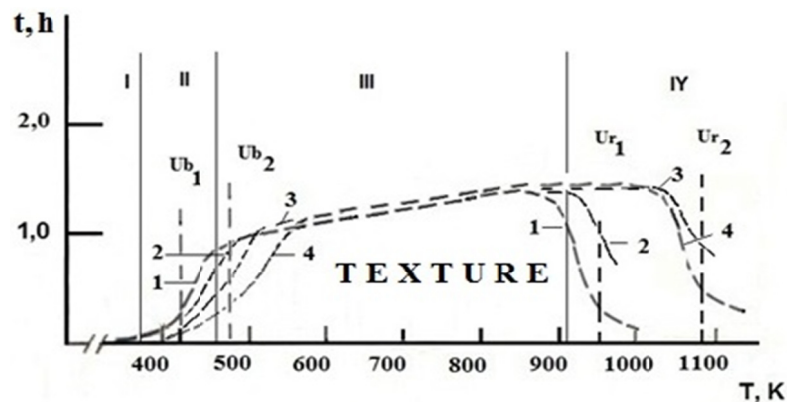

Figure 8. Dependence of durability of coatings based on dichalcogenide on Al$_2$O$_3$ specimens on substrate temperature during triboengineering tests of disk-on-sphere couples: (1) MoS$_2$; (2) MoSe$_2$; (3) WS$_2$; (4) WSe$_2$

The range of crystallization of MoSe$_2$, WS$_2$, and WSe$_2$ shifted to the zone of higher temperatures, the highest temperatures of transition from the amorphous structure to the textured crystalline structure were demonstrated by the tungsten diselenide WSe$_2$, and it accompanied by the relevant shift to higher triboengineering characteristics in the region of higher temperatures (Figure 8). This is apparently due to the shift in the surface energy U$_b$ potential barrier towards the range of higher temperatures. This shift reduces the crystallization region width; the narrowest crystallization range belongs to MoS$_2$ (473–523 K), the widest one belong to WSe$_2$ (493–563 K). This phenomenon was discussed by Nozhenkov (2012b, 2013a, 2014).

To assess the effect of material hardness, the substrate was coated with MoS$_2$ by high-frequency sputtering at a temperature 523 K on the specimens from 12X18H10T steel (with a Vickers hardness HV of 179 kgf/mm^2), SH -15 steel HV = 760–800 kgf/mm^2 (Rockwell hardness was 62–63 HRC), and a compact corundum ceramic Al$_2$O$_3$ (with HV = 2060 kgf/mm^2 [Moos hardness was 9]).

The accomplished friction tests of disk-on-sphere couples and end-face friction tests (Figure 9) showed a much lower coefficient of friction when testing disk-on-sphere couple versus end-face tests; it is apparently due to the higher specific loads in the contact zone. It also follows from test results that the best coefficient of friction and durability belong to the specimens of compact ceramic Al_2O_3, while the poorest one belongs to the specimens from 12X18H10T with the least hardness. The result of the specimens from SH-15 steel showed mediocre values. The papers (Nozhenkov, 2012a, 2012b, 2013a, 2014) show that the harder the substrate, the smaller the coefficient and the more operating life the coating. This relates to the coatings based on the dichalcogenide and can be explained by the easy splitting and orientation of crystallites in the process of friction.
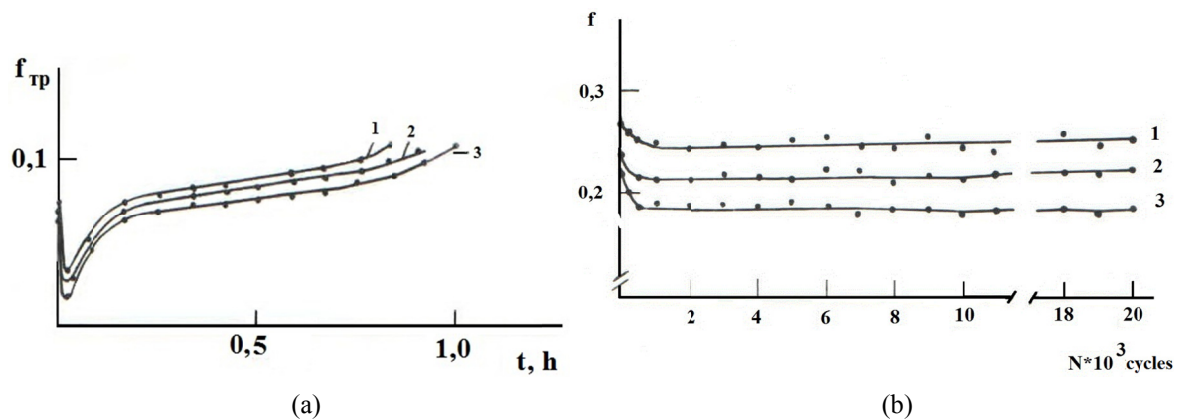

(a)   (b)

Figure 9. Dependence of coefficient of friction on duration of tests of MoS_2 coatings 0.5 µm thick applied on specimens of (1) 12X18H10T steel, (2) SH-15 steel, (3) Al_2O_3 compact ceramic: (a) disk-on-sphere couples (UGS-1); (b) end-face friction couples (MPC-1)
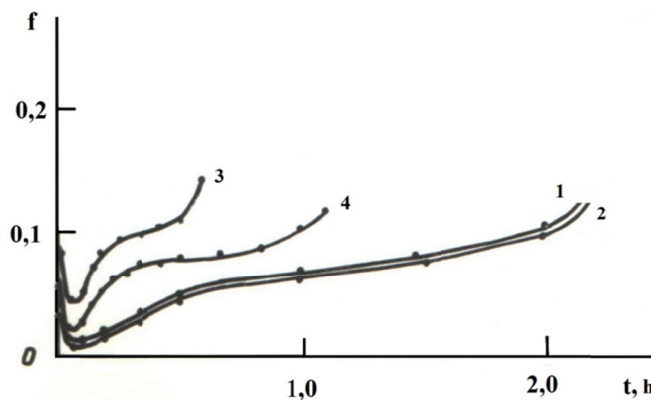

Figure 10. Dependence of the coefficient of friction on the time (h) of testing MoS_2 with a thickness of 0.5 µm applied to a (1, 3) direct current and (2, 4) high sputtering with (1, 2) and without (3, 4) a negative potential displacement of 50 V. Disk-sphere testing scheme in air

2.4 Effect of the Potential Applied to the Target, and the Negative Substrate Bias Potential on the Tribological Characteristics

To check the chances of improving the tribotechnical characteristics by modifying the process of application of coatings, the coatings based on the molybdenum disulfide applied at various potential types to the target (constant and high frequency), and by feeding negative shift potential (up to 100 V) to the substrate during application. It was established that changes in the highfrequency discharge versus DC sputtering, which adds a slight negative bias potential (up to 100 V) to the substrate during application improves the triboengineering properties of coatings from molybdenum disulfide.

The accomplished improvements in work of the technology and friction tests of MoS_2 coatings applied by high-frequency sputtering with bias demonstrated a higher growth of the bias potential from 0 to −30 V, which improves the triboengineering characteristics of the applied coatings versus the properties of the same coatings

MoS_2, yielded high-frequency sputtering without displacement (Figure 9).

The stabilized coefficient of friction values diminish, while the durability extends. At a bias potential of −30 to −50 V, the best tribotechnical characteristics were obtained; a further rise in the bias potential to -100 V does not improve the characteristics. Work (Nozhenkov, 2013b) relates the improvement of the tribotechnical characteristics to the essential introduction of argon atoms into the dichalcogenide lattice. Therefore, the present paper deals with MoS_2 coatings applied by high-frequency sputtering using a negative bias potential of 50 V and friction tests. The results of triboengineering tests are shown in Figure 10.

An analysis of the electronogram demonstrates that molybdenum disulfide applied by sputtering with a shift increases the lattice period along the c axis by $12.8–13.3×10^{-10}$ m, instead of $12.295×10^{-10}$ m, and the stoichiometric $2H-MoS_2$. Apparently, the application of MoS_2 with the superposition of the negative shift potential in these coatings augments the argon content. This may be due to the additional flux of positively charged argon ions that bombard the negatively charged coating surface. Thus, one of the reasons of different tribotechnical characteristics of MoS_2 coatings applied by usual sputtering and by feeding negative bias potential from −30 to −120 V may be the lack of argon atoms in the crystalline lattice of the hexagonal $2H-MoS_2$. The argon atoms should apparently be located in spaces between packs of S–Mo–S because it is rather unlikely that they would be located within packs where there is dense hexagonal packing. The location of argon atoms in spaces between S–Mo–S packs should lead to a significant reduction in the interlayer interaction. In addition, the surface cleaning of applied coatings with argon ions favors the quality and improves the MoS_2 lubricity and quality. Thus, molybdenum disulfide is doped with additional element atoms (argon). However, the argon content in the coating can be increased to a certain limit. The bias potential above −120 V distorts the MoS_2 crystalline lattice by intensive ion bombardment and growth of crystallites, which strongly impairs the lubricity of molybdenum disulfide coatings.

2.5 Alloyed Coatings

Doped coatings of molybdenum disulfide composition MoS_2D_x were deposited (Nozhenkov, 2012a, 2012b, 2013a, 2013b, 2013c, 2014), which in appearance is not much different from the usual sputtered thin films MoS_2. As the dopant D may be selected elements or compounds which do not form strong (chemical) bonds with the main grating MoS_2. In friction tests Disk-sphere testing scheme services coating hexagonal crystal structure of molybdenum disulfide $2H-MoS_2$ were obtained sufficiently low coefficient of friction, but generally corresponding to the friction of natural molybdenum disulfide.

However, friction tests under the same conditions coating composition MoS_2D_x led to the production of unusually low values of the coefficient of friction on the air under normal conditions (the phenomenon of ultra-low [or super-low] friction, Figures 11, 12).

Electron diffraction studies of coatings MoS_2D_x showed that there was a significant increase in the lattice along the c (max. 1.38–1.43 nm against 1.2295 nm) for compounds with a stoichiometric composition (hexagonal $2H-MoS_2$) in practically constant period along the a axis. Increasing the distance between the layers when placing the D atoms in the inter-packet spaces in view of the fact that the energy of the van der Waals interaction varies with the $\sim r^{-6}$ shall be led to a reduction of this interaction is practically an order of magnitude.
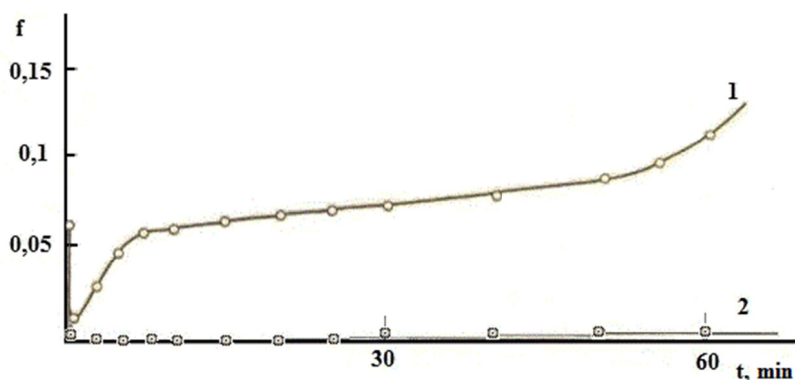

Figure 11. The dependence of the coefficient of friction on time (min) of tests of the doped MoS_2 coatings on Al_2O_3 on the air under normal conditions: 1–MoS_2; 2–MoS_2D_x
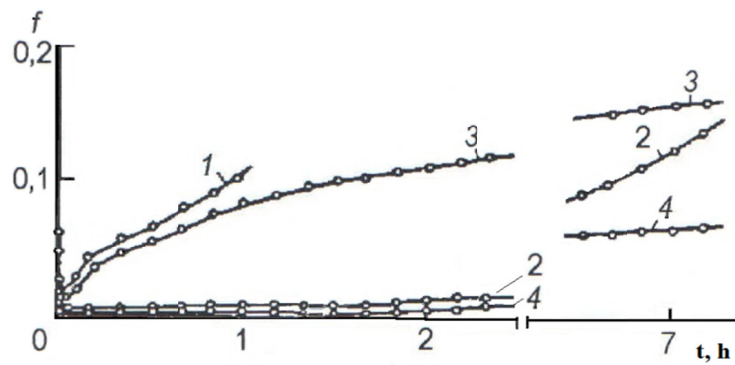
Figure 12. Dependence of coefficient of friction on time of tests of coatings on the air under normal conditions: (1) MoS_2; (2) MoS_2D_x; (3) ($Mo_2N–M_kN_mX_n–MoS_2$); (4) ($Mo_2N–M_kN_mXn–MoS_2D_x$).

(a)   (b)

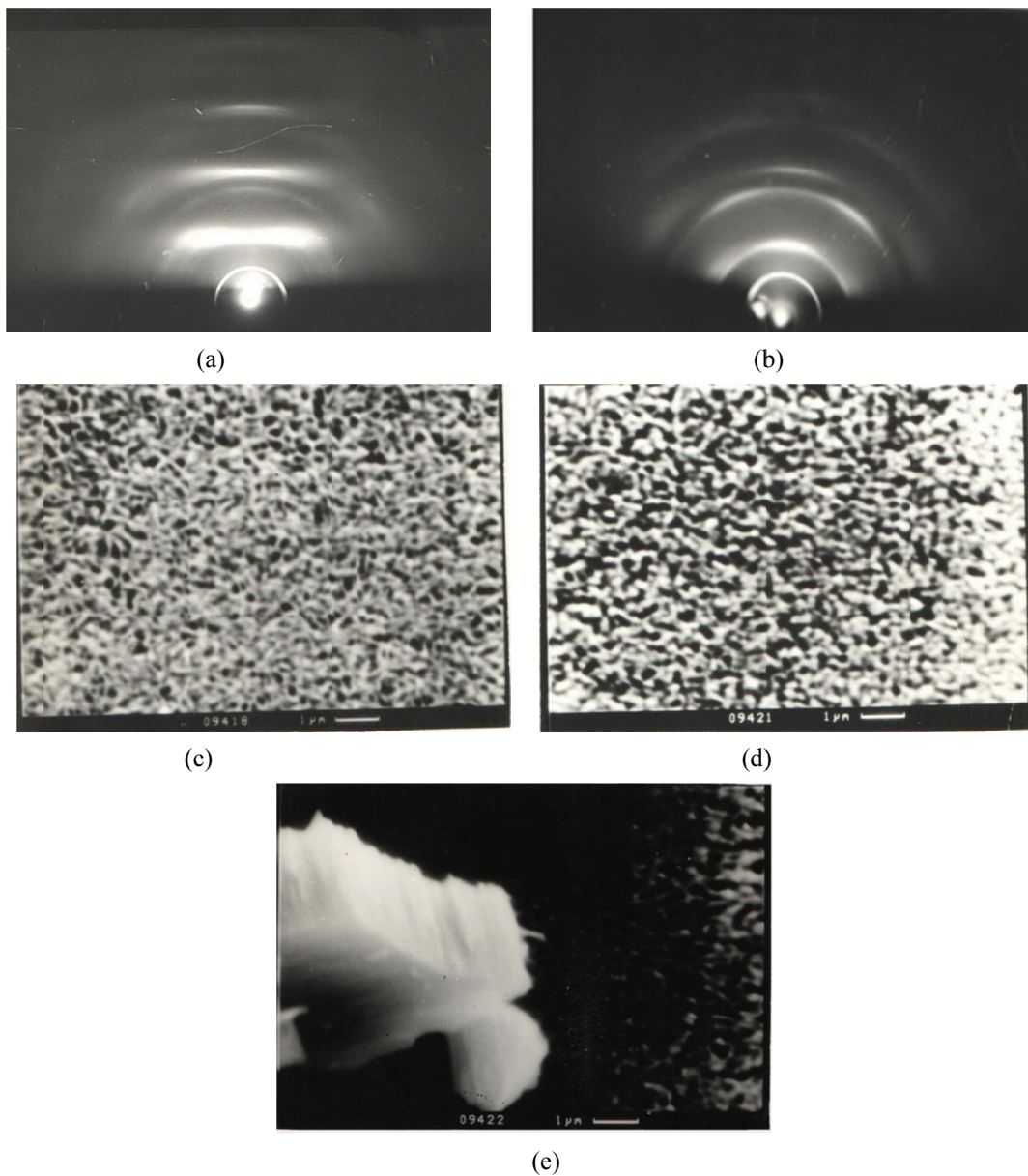(c)   (d)

(e)

Figure 13. Electronograms (a, b) and microphotographs ($\times$5000) (c, d, e) of WS_2Ga_x coatings and WS_2Ga_x coating step, when specimens are located in center (a, b) and periphery (c, d) of plate
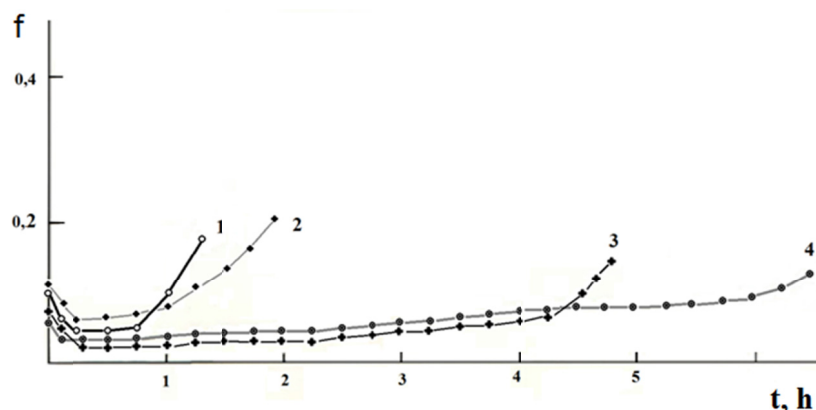
Figure 14. Dependence of coefficient of friction on time of tests of WX_2 coatings and doped WX_2Ga_x coatings with wear-resistant Cr_2O_3 sublayer applied on titanium alloys. Tests on disk-on-sphere scheme: (1) WS_2; (2) WSe_2; (3) WSe_2Ga_x; (4) WS_2Ga_x

2.6 Anti-Friction Coating with Wear-Resistant Underlayer

It is shown above that a harder substrate facilitates the spalling of crystallites and formation of the predominant orientation [0001] on the friction surface. Hence, the further improvement of the triboengineering properties can be achieved by applying a wear-resistant sublayer. In addition to the wear-resistant sublayer, the improved triboengineering characteristics are achieved by doping the molybdenum disulfide with extra element atoms (Nozhenkov, 2012a, 2013a, 2014). Consecutive studies of composite wear-resistant composite antifriction coatings with the variable composition thickness from the wear-resistant to the antifriction layer ($M_kN–M_kN_mX_n–MX_2D_x$) that contain the element N (e.g., nitrogen) are responsible for the strength and wear resistance of the whole composition, changes from the optimum to zero, while the halcogen H increases from zero to the stechiometric content. In addition this composite can be doped with additional element D_x (such as X or Ga). These coating were obtained by using the shift potential and delivery of reactive gas into the vacuum chamber during coating application on the specimens from steel 12X18H10T.

The triboengineering tests have demonstrated that the composite coatings possess high antifriction properties. The application of the MoS_2 coating with the transitional $M_kN_mX_n$ layer and the Mo_2N sublayer on specimens from stainless steel 12X18H10T enables on to improve the triboengineering properties of friction couples. The shift potential during the application of coatings considerably improves the triboengineering properties apparently due the different placement of argon atoms in the dichalcogenide crystalline lattice; it increases the spacing of chalcogen–metal–chalcogen packs and facilitates spalling and consecutive sliding in friction, which ensures ensuring the effect of bidimensional gas on surfaces (0001) dichalcogenide crystallites. This is why the shift potential and the reactive gas delivery into the vacuum chamber served to apply composite coatings with the content variable rough thickness from the wear-resistant to the antifriction layer ($M_kN–M_kN_mX_n –MX_2D_x$) in which the outer antifriction dichalcogenide layer of the stechiometric composition was replaced with the MX_2D_x layer, which has the additional doping element D_x. The application of the MoS_2D_x coating yields an ultra low coefficient of friction in air under normal conditions (Figures 11, 12).

The application of the wear-resistant Mo_2N sublayer with the transitional $M_kN_mX_n$ layer and the antifriction MoS_2D_x layer enables one to considerably improve the tribological properties of the entire composition and to effectively protect the working surfaces of friction couples, in particular those from stainless austenite steel.

Composite wear-resistant antifriction coatings based on molybdenum and tungsten disulfide and diselenide WS_2 and WSe_2 applied on the specimens of constructional titanium alloy VT23 were studied. These titanium specimens were first provided with the wear-resistant sublayer of Cr_2O_3 by REB (Nozhenkov, 2012a, 2013a, 2014) 2.0–2.5 mkm, then the high-frequency cathode sputtering applied WS_2 and WSe_2 to Cr_2O_3; they were also additionally doped with gallium (Ga) on the WS_2Ga_x and WSe_2Ga_x coatings. The results electronographic and electron microscopic studies are represented in Figures 6, 7, and 13. The WS_2 and WSe_2 coatings based on dichalcogenide had the hexagonal $2H–MoS_2$ structure. The tribotechnical characteristics were quite high; in general, they corresponded to the friction of the natural molybdenum disulfide (Figure 14).

The doping of the WS_2 and WSe_2 with extra gallium (Ga) that produces alloyed WS_2Ga_x and WSe_2Ga_x coatings would considerably improve the durability of these coatings (Figures 15, 16). It should be noted feature of the

motion of the particles of the doping elements (atoms, molecules, clusters) in the absence of external influences and turning them into the inertial reference system. These particles have the possibility movement on a solid surface uniformly, without dissipation of energy, that is the possibility of zero change of the interaction energy with the surface of a solid body in motion. The most likely implementation of such a phenomenon on singular plane (0001) with the realization of ultra-low (zero) friction without energy dissipation, in the absence of resistance forces the process of moving.

The obtained results of improving the tribotechnical characteristics and the mechanism of growth of crystallites with planes (1010) and (1120) of the crystallites with hexagonal (110) and cubic structures that were almost perpendicular to the flow of deposited particles can be explained using the model developed in Nozhenkov (2012a, 2012b, 2013a, 2013b, 2013c, 2014) and Ginzburg (2000). These works consider the process of the formation of condensed solid body from the flux of atomized particles, and a model is proposed for crystallite growth due to the possibility of the diffusive migration of deposited atoms on the growing coating surface and the creation of mobile particulate monolayers on dichalcogenide packs of the two-dimensional gas during the friction of the obtained doped coatings.

This migration of particulate monolayers is possible when the heat energy of the particles exceeds the surface-potential barriers. The mobile particles reduce the interaction between chalcogen–metal–chalcogen packs, and facilitate the mutual sliding of dichalcogenide packs. This will be shown in the following.

3. Mechanism of Ultra-Low Friction

Features of the crystal structure and anisotropy caused use for various purposes, the materials with laminated (lamellar) structure, for example, transition metal dichalcogenides. It is a crystalline substance with a lamellar structure in which together with the strong ionic-covalent interactions between the atoms in the individual lamella are weak van der Waals forces between adjacent layers. Transition metal dichalcogenides metal finish building the d-electron is consisted the associated by weak van der Waals packages chalcogen-metal-chalcogen (X-M-X), within which there are strong exchange interactions formed complex ion-covalent bonds with applying metal interactions in the center of the package. For example, molybdenum disulfide (α-MoS$_2$), wherein the bivalent and tetravalent molybdenum sulfur have electronic configuration Mo^4-4d^{5}5s; S^2-3s^{2}3p^4 with ionic radius for Mo^{+4}-0.068 nm for the S^{-2}-0.182 nm there exists in the hexagonal crystal system.

In the formation of bonds involved dsp-orbit. In the molybdenum disulfide is d^{4}sp-hybridization, i.e. ties involved in the formation of 4d-, 5s- and 5p-electrons of the central atom, and the only one not involved in the communication orbit molybdenum atom is occupied by two electrons. Interactions between packets have the dispersion nature, which are based on instantaneous dipoles formed by the action of the collective phonon vibrations of the atoms inside the package X-M-X. These vibrations cause additive phonon vibrations associated with the polarization of opposite sign in the next package. The additivity of the dispersion interaction causes his long-range nature and potential of this interaction decreases with increasing size of the gap by doping dichalcogenide by law r^{-2}.

In the study of changes in surface layers dichalcogenides during sliding above it was found that the initial structure with a preferred crystal orientation (texture) with the [1010] is converted into the texture with the [0001] direction perpendicular to the substrate. The implementation process of the shift and further slip planes basis (0001) for each other is the most energetically favorable and occurs at the lowest cost to the relative movement of solids. The determining factor in this process is to not break the binding energies of Ur in the contact area, and the shift of the atomic planes with overcoming potential barriers, sliding over each other surfaces U$_b$.

Established (Nozhenkov, 2012a, 2012b, 2014) that the occurrence of ultra-low friction due to the presence of migrating phase on friction surfaces in a state of two-dimensional gas. In this phase, the particles (atoms, molecules, clusters) can be adsorbed from the environment or introduced in the solid lattice when shaping it. For very low coefficients of friction in normal conditions the air to shift the phase transition in the temperature range less than 300 K, ie, the binding energy of atoms adsorbed on the (0001) dichalcogenide for free migration on the surface to be less than the kinetic energy of the atom under normal conditions. Moving the masses without the heat loss can be along the lines of equipotential surface field. Moving across the lines of equipotential field is accompanied by energy costs to heat dissipation. The presence of the alloying particles monolayers on friction surfaces increases the distance between the (0001) planes (Figures 17, 18) and reduces the energy of the interaction between layers U$_r$. Such particles in the case of the possibilities for diffusion migration to the surface (0001) provide ease of sliding of the opposite surfaces (0001) and thus to move in the particles along the equipotential field lines of the surface (0001) there is possibility of movement without energy dissipation.
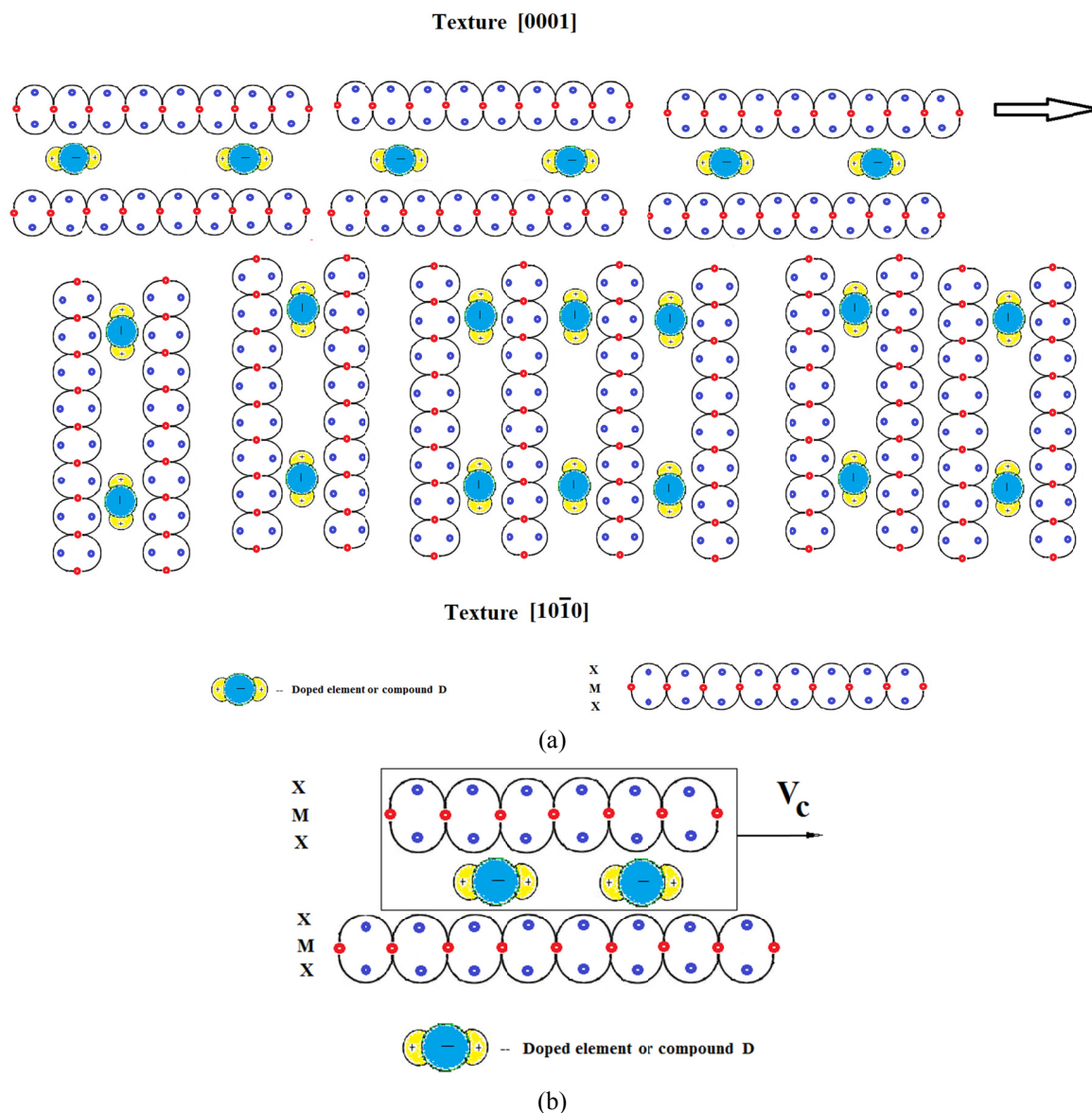
Texture [0001]

Figure 15. Doped coatings based dichalcogenides MX_2 (M - metal, X - chalcogen) with texture [10$\bar{1}$0] and the appearance of the upper layers of texture [0001] (a), the formation of an inertial frame of reference on the equipotential surfaces (0001) dichalcogenide moving with speed V_c uniformly without any loss of energy (b)

Based on the studies can offer a range of properties for ultra-low friction of a layered anti-friction materials. For the lowest values of the coefficient of friction is necessary to the formation of the crystalline (non-amorphous) structure dichalcogenide. The structure dichalcogenide in interlayer space must be atoms or molecules intercalated materials having weak interactions with surfaces (0001) dichalcogenide. Among themselves, such atoms (molecules) should also not have strong ties. By increasing the lattice constant along the C axis, the intercalated material provides ease of cleavage and further layers dichalcogenide slip relative to each other. It should be noted that during friction is even greater distance between the planes (0001) and the gap width is determined by the attraction and repulsion potentials determined by the equation of Lennard-Jones potential. The particles of matter are intercalated in the gap between the planes with the corresponding change in the time of sedentary life and move in concert with the package dichalcogenide as a single inertial system.
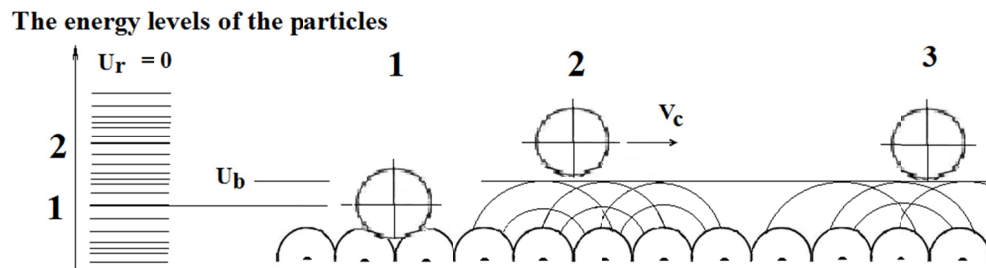
Figure 16. Move adsorbed atoms on the surface at the time jump from position 1 to position 3 the atom is in a two-dimensional gas

High tribological properties of the coatings on the basis of the dichalcogenides in the process of friction are determined easily splitting the crystals along the (0001) dichalcogenide packages where there are weak van der Waals interactions of the type not associated with the exchange or sharing of electrons, and further sliding of packages each other. In this case, the hardness wear-resistant underlayer promotes an orientation and magnitude of the coefficient of friction depends on the interaction energy between the layers dichalcogenide. Let us consider the phenomena occurring in the contact zone of the samples.

In Nozhenkov (2012b, 2013a, 2013b, 2013c) established a generalized mathematical model of the process of application and prediction derived properties of ion-plasma coatings, which determines their structure during application and physico-mechanical properties of the application of such coatings. Representation of the model is related to the possibility of diffusion migration of particles on the surface of a solid. A monolayer of particles deposited in each sufficiently small (compared to the monolayer deposition time) period of time can be represented as two phases condensed, which are particles with heat energy less than the potential barrier and are responsible for the formation of a disordered (amorphous) phase, and migrates to include particles capable of migrating to an atomically smooth surface areas. This migration occurs in the case of excess heat of adsorption particles magnitude of potential barriers to the surface. The clash with the defect (for example, a step) leads to an increase in the potential barrier in two or more times, which should, according to

$$\tau = \tau_0 \ e^{-U_b/kT} \tag{1}$$

where τ_0 is time thermal vibrations, U_b is the energy of the potential barrier, kT is the thermal energy of the particles. Atoms in the adsorption sites are in a settled state of the condensed phase. Migratory phase can be represented as a two-dimensional gas on the surface, which is to obey an exponential distribution (Maxwell distribution) particle energy. The ratio of the two phases determines the structural condition of the growing surface. Then the crystal size L in the growing coverage in (Nozhenkov, 2012b, 2013a, 2013b, 2013c, 2014) is defined by the ratio of the condensed phase (defined by B), and the migratory phase (defined by C).

$$L = A \ [(1-\varepsilon)B+\varepsilon C]^{1/2} \tag{2}$$

where the A is value depending on the structure and properties of the deposited material, ε is coefficient Maxwell distribution of energy.

When coating a possibility of making additional dopants into the crystal lattice of the growing coating (effect intercalation). In the process of friction intercalated particles of the coating after splitting the crystals into the state of two-dimensional gas on surfaces (0001) dichalcogenide. Then for ultra low coefficient of friction requires a certain amount of additional substances as particles (atoms, molecules, clusters) of the crystal surface and the displacement of the phase transition to a temperature less than 300 K, i.e. the binding energy of atoms adsorbed on the (0001) dichalcogenide for free migration on the surface to be less than the kinetic energy of the atom under normal conditions.

If the settled life (1) of the adsorbed atom in the potential well, where it has taken hold, is greater than the monolayer deposition time, such an atom is immured subsequent monolayers in the growing surface. In the first step of the clusters are formed, which are attached to the deposited atoms. The coating of the surface at a high enough temperature the particles are sorted by potential holes according to their thermal energy and healing of defects migrating particles to form a sufficiently large number of atomically smooth surfaces. Migratory phase can be represented as a two-dimensional gas on the surface obeys the Maxwell distribution. Then the Equation (2)

$$L = a/d \ [(1-\varepsilon) \ v_m\tau_0/v_n\tau_n \ e^{U_b/kT} + \varepsilon \ v_m/v_n)]^{1/2} \tag{3}$$

where a is the lattice material applied coating; d is number of obstacles migration of atoms on the surface of the growing crystal (steps, vacancies, colliding atoms); $V_m = (3kT/m)^{1/2}$ is thermal migration rate, k is Boltzmann constant, T is temperature K, m is mass of the atom; $v_n = h_n/\tau_n$ is the growth rate of coverage (about 1–10 monolayers), h_n is coating thickness, τ_n is coating time, τ_0 is time thermal vibrations of atoms, U_b is the potential barrier surface, ε is the number of particles with energies exceeding a surface potential barrier (varies with increasing temperature from 0 to 1). The durability of coatings may be determined as a function of crystal size t = kL, where k is proportionality factor.
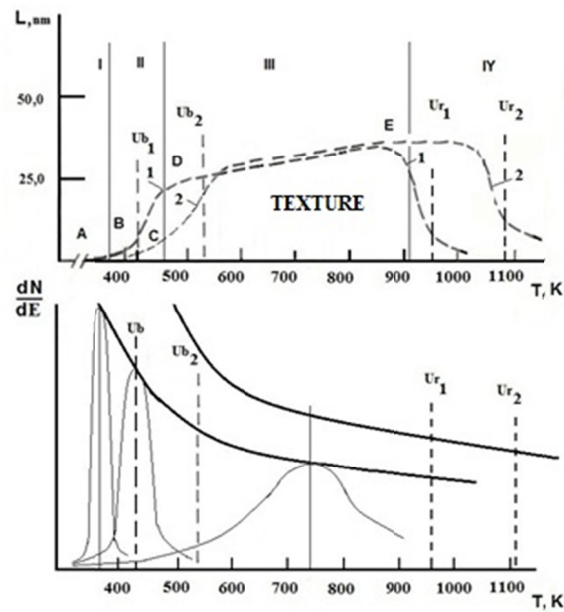

Figure 17. Dependence crystal size (a) and the energy distribution of particles (b) of the substrate temperature for the metal compound-chalcogen MH_2 (1 or 2)

Curve 1, 2 is Coating crystal size MH_2 of compound (1 or 2); Curve 3, 4 is the envelope of the inflection points of the energy distribution of particles connection MH_2 (1 or 2); $U_{b1,2}$ is a potential barrier surface connection MH_2 (1 or 2); $U_{r1,2}$ is energy of the particle compound MH_2 (1 or 2); A is point polycrystalline growth phase B is the inflection point on the temperature of the crystal size; D is starting point of growth textured coating, E is starting point of decomposition coating on metal and chalcogen.

Growth of crystals with increasing temperature transition represents the distribution function of the surface potential barrier occurrence c of the phase transition of investigated crystallization temperatures to form a coarse structure coatings.

Consequently, the ratio of the two phases on the surface determines the structure formed by the applied coating. Crystal growth with increasing temperature is the transition of particles obeying the distribution function through the potential barrier surface. With this move particles through a potential barrier is related sharp increase in the size of the crystals in the crystallization (Figure 16). In the field of condensed matter (curve segment AB), designated by the numbers I, formed mainly amorphous structure, which is responsible for particles of a condensed phase. In this case, the deposited particles are fixed in random places collision with the surface of the growing coating and thus is a normal crystal growth mechanism. In the field of migrating particles (curve segment DE, III) is realized mainly step mechanism of crystal growth. In the transition region (the segment of the curve II) is increasing the number of migratory phase, followed by increasing the size of crystallites. At the inflection point of the envelope (line 3 and line 4) marked point with the potential barrier U_b, point E is energy of Ur, above which a re-evaporation (or decomposition) of deposited particles.

The experimentally observed broadening of the distribution curve of the particle energy with increasing temperature (Figure 3) is connected, apparently, with an offset value of the potential barrier U_b to higher temperatures. Such a shift leads to an increase in the width of the crystallization, the minimum width of the crystallization at the MoS_2 (473–523 K), the largest in WSe_2 (493–563 K).

4. Discussion of Results

It should be noted that the phenomenon of superconductivity and ultra low friction was observed in the crystal structures of layered dichalcogenide type (MX$_2$) and diboride (MB$_2$) metals (M: metal; X: chalcogen; B: boron) (Bulaevskii, 1975; Ginzburg, 2000; Kirzhnits, 2001). It is a crystalline substance with a lamellar structure in which the on—line with the strong ionic-covalent interactions between the atoms in the individual lamellae of (layers) are weak van der Waals forces between adjacent layers. For example, transition metal dichalcogenides metal finish building the d-electron shells are composed of—span of the associated by weak van der Waals packages chalcogen-metal-chalcogen (X-M-X), within which there are strong exchange interactions formed complex ion-covalent metal overlay communication interactions in the center of the package. For example, molybdenum disulfide (α-MoS$_2$), wherein the bivalent and tetravalent molybdenum sulfur have electronic configuration Mo^4-$4d^5 5s$; S^2-$3s^2 3p^4$ with ionic radius for Mo^{+4} 0.068 nm, for the S^{-2} 0.182 nm—there exists in the hexagonal crystal system. In the formation of bonds involved dsp- orbit. In the molybdenum disulfide is d4sp- hybridization, ie ties involved in the formation of 4d-, 5s- and 5p-electrons of the central atom, and the only one not involved in the communication orbit molybdenum atom is occupied by two electrons.

Interactions between packets have the dispersion nature, which are based on the dipoles formed by the action of the collective phonon vibrations of the atoms inside the package X-M-X. These vibrations cause additive phonon vibrations associated with the polarization of opposite sign in the next package. The additivity of the dispersion interaction (as opposed to binary interactions of exchange type) causes his long-range nature and potential of this interaction decreases with increasing size of the gap by doping dichalcogenide by law r^{-2}.

High-temperature transport of mass (energy) without dissipation (heat dissipation) is possible along the lines of equipotential surfaces (0001) anisotropic layered compounds in the presence of a layered structure of solid spaces van der Waals forces. Owing to the special condition of the layered solid—the availability of space Van der Waals forces—which are long-range dispersion forces, and there are no free valence electrons capable of forming a strong exchange interactions, there is a possibility of moving particles without dissipation (scattering) of energy. Dissipative processes are the result of the forces of resistance arising in the metabolic processes of interaction. The strength of the resistance movement occurs in the case of change of speed of movement (the emergence of the acceleration) at the intersection (movement across) the force lines of the equipotential field

$$F = ma = m \, dV/dt \tag{4}$$

Figure 16 shows that for the migration of the particles on the surface (0001) Solid State must inform the latter of the diffusion activation energy to overcome the potential barrier surface, the activation energy does not exceed the energy of the particle and the surface to avoid desorption (reispareniya) particles from the surface. Requires the creation of conditions for the migration of the particles (using the appropriate temperature of the friction pair) and freezing of high energy particles (photons, phonons), resulting in a two-dimensional gas desorption, which provides ultra-low friction.

In the study of the transfer of electric charges and the atoms of helium at low temperatures observed phenomena of superconductivity and superfluidity (Bulaevskii, 1975; Ginzburg, 2000; Kirzhnits, 2001). The basis of these physical phenomena is the formation of Cooper pairs of electrons and superconductivity or of helium-3, with superfluidity, which leads to a lack of heat loss with the flow of the particles and the disappearance of the friction between the moving particles and the lattice of a solid. Electrons and nuclei of helium-3 are fermions with half-integer spin ½. The atoms of the isotope helium-3 (helium ^{3}He) are fermions, but at sufficiently low temperatures combined into Cooper pairs with integer spin, representing bosons. Fermion through a field directly interacts with another fermion with the emission of a photon and form a boson with integer spin. The emission of a photon in the process of formation of the Cooper pairs—the radiation of excess energy when two electrons, like the rays of the electron and proton in a hydrogen atom to form an integral particles, as discussed in (Nozhenkov, 2012b). Formation boson happens to the radiation of energy education, the decay with the corresponding radiation. To save the opposite curvature of Riemann and Lobachevsky fields in the hydrogen atom emission occurs on the outside of the atomic electron's orbit, and in a Cooper pair from the center, located between the electrons. The radius of curvature of the mass of a photon emitted by a hydrogen atom, is equal to the radius of the main orbit of the hydrogen atom, de Broglie radius of a photon emitted by a hydrogen atom in the ground state, in 1/α times the radius of the mass of the photon. The size of the Cooper pairs is proportional to the fine structure constant α and the diameter of the main orbit of the hydrogen atom. Formed by a Cooper pair is stable, resistant and has the ability to move in the lattice of a solid at zero-point oscillations of the atoms of the latter without energy dissipation. For the destruction of the Cooper pairs (the creation two fermions of one boson) particles are needed with the appropriate energy E$_f$, which is the activation energy of decay and

numerically equal to the energy of formation of boson. The destruction of the Cooper pair without decomposition activation energy is impossible. The task of maintaining the Cooper pairs in a stable condition for high-temperature superconductivity is to absorb particles (photons, phonons) c energies equal to the corresponding activation energy of decomposition Cooper pairs. Emerged after the collapse of bosons fermions are scattered by the crystal lattice of the solid (phonons, lattice defects) with the dissipation of energy, which creates obstacles to their free movement and the movement of the particles is carried out with the presence of heat dissipation.

The intercalation enhances the superconducting properties of dichalcogenides (Bulaevskii, 1975) and in certain circumstances, allows you to get ultra-low friction phenomenon (Nozhenkov, 2012a, 2012b, 2013a, 2013b, 2013c, 2014). The arrangement of atoms of doping element in the van der Waals interlayer spaces accompanied by the formation of two-dimensional electron gas. The electrons of a Cooper pairs move in two parallel spaces van der Waals forces between the layered material packages. When creating the appropriate conditions in a layered crystal structure with high anisotropy properties formed Cooper pair can exist long enough under normal conditions. In the papers (Nozhenkov, 2012b, 2014) that this stability of the particles and the lack of heat dissipation (in the form of photon emission) is ensured by the proportionality of the geometric structure of the particles of the fine structure constant α.

Accordingly can imagine superconducting and superfluid state of matter with the help of Equations (2), in which the properties of a substance depend on the proportion of the two phases. Superfluidity and superconductivity, which can be regarded as the superfluidity of the electron gas are related phenomena, as well as ultra low friction, determined by the mobility of two-dimensional gas of particles.

Consequently, in the case of superconductivity and superfluidity applied for the emergence of ultra-low friction ratio (17) can be represented as the ratio of normal and superconducting (or superfluid) phase with the corresponding phase transition as a transition curve of particle energy (Equations 2, 3) through the critical value (potential barrier critical temperature)

Properties of the substance depend on the proportion of the two phases, and the change of state is seen in the case of superfluidity as a phase transition of type II normal liquid 4He and 3He in superfluid He II (Bose condensation). Then Equation (4) can be regarded as the ratio of the two phases in the two-fluid hydrodynamics Landau

$$K_{sf} = k_{sf}L_{sf} = k_{sf}A \ [(1-\varepsilon)B_{HeII} + \varepsilon C_{He}]^{1/2} \qquad (5)$$

where ε is the coefficient of particle energy; B_{HeII} is the number of particles of the Bose-condensate, C_{He} is the number of particles of normal liquid ^4He and ^3He; A is the value depending on the structure and properties of the deposited material; K_{sf} is the relative magnitude of the forces of resistance movement of the fluid particles. In the case of superconducting phase transition occurs in the normal electrons in a Bose condensate of Cooper pairs of the superconducting phase (Figure 18):

$$K_{SC} = k_{SC}L_{SC} = A \ [(1-\varepsilon)B_{SC} + \varepsilon C_n]^{1/2} \qquad (6)$$

where B_{SC} isthe number of particles of the superconducting phase Bose, C nisthe number of particles of normal conduction electron phase; K_{SC} is the electrical resistance of the test substance, respectively, growing with increasing temperature T.

Consequently, in the case of superconductivity and superfluidity Equations (2, 3) can be represented as the ratio of the normal and superconducting (or superfluid) phase with the corresponding phase transition of the energy distribution of particles over a critical value (a potential energy barrier), as in the case of ultra-low friction, which is related phenomenon (Figure 17).

Therefore, the phenomenon of non-dissipative movement of mass (energy) along the lines of equi-potential fields, which manifests itself in the form of ultra-low friction, superconductivity and superfluidity of matter can be under normal conditions between the surface of solid along the force lines of equi-potential field, determined by the shape and value of the Fermi surface in k-space. In this energetically favorable arrangement of the particles in the crystal lattice for the realization of the non-dissipative movement with the disappearance of forces of resistance are van der Waals areas, which are followed to predict the possibility of the appearance of the investigated phenomena.
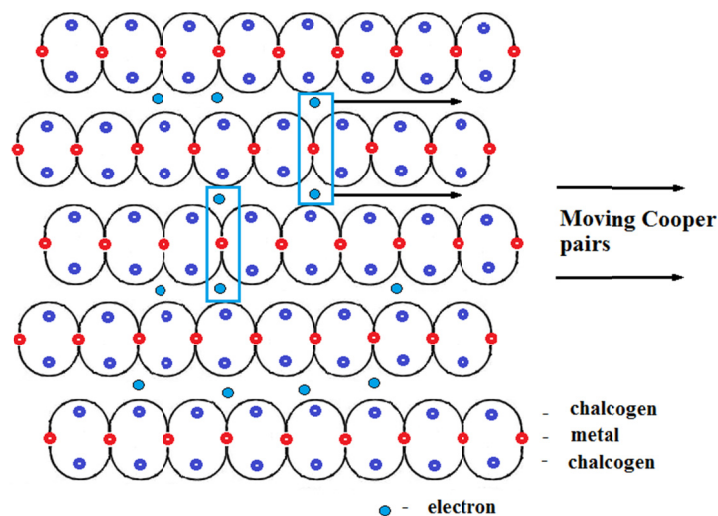
Figure 18. Formation and movement of the Cooper pairs in the interlayer spaces of the layered structure

5. Conclusions

1) It is shown that the highest tribological properties are coatings based on transition metal dichalcogenides crystalline structure, an amorphous structure with a coating as antifriction practically inapplicable.

2) Created composite coatings of variable on thickness of the composition of the wear layer to doped anti-friction with high-protective anti-friction and anti-wear properties;

3) Doped coating enables obtaining ultra-low (super-low) friction under normal operating conditions in air and leads to an increase in the durability of the coating multiple times.

4) Found that the ultra-low (super-low) friction, superconductivity and superfluidity are related phenomena defined phase transition particle energy distribution across the critical value (energy potential barrier).

5) The generalized mathematical model of the process of application and obtained the properties of ion-plasma coatings, which determines the mechanical properties of the application of such coatings.

References

Bulaevskii, L. N. (1975). Superconductivity and electronic properties of layered compounds. *UFN, 116*(3), 449-481. http://dx.doi.org/10.3367/UFNr.0116.197507c.0449

Ginzburg, L. (2000). Superconductivity. Yesterday, today and tomorrow. *UFN, 170*(6), 619-630.

Kirzhnits, D. A. (2001). Statistical model substance, superconductivity and superfluidity, cosmology and astrophysics. *Proceedings in theoretical physics, 2*, 432. Moscow: FIZMATLIT.

Nozhenkov, M. V. (2012a). On low interaction of particles in solids. *Nanoinzheneriya, 3*, 41-48.

Nozhenkov, M. V. (2012b). Crystal structure and properties of coatings superimposed by vacuum ion-plasma methods. *Strengthening Tekhnology&Coatings, 9*, 38-48.

Nozhenkov, M. V. (2013a). Technology and application properties of vacuum ion-plasma coatings. *Friction & Lubrication in Machines and Mechanisms, 7*, 3-12.

Nozhenkov, M. V. (2013b). Equipment for the application wear-resistant anti-friction compositions. *Friction & Lubrication in Machines and Mechanisms, 8*, 20-28.

Nozhenkov, M. V. (2013c). On the ultra-low friction layer structures. *Friction & Lubrication in Machines and Mechanisms, 11*, 3-12.

Nozhenkov, M. V. (2014). The structure and properties of vacuum ion-plasma coatings. *Journal of Surface Investigation. X-ray, Synchrotron and Neutron Techniques*, 1.

Copyrights